Proc. Indian natn. Sci. Acad., **60**, A, No. 3, 1994, pp. 361-392.
©Printed in India

ATMOSPHERIC CLIMATE MODELLING—A VIEW OF CURRENT ACTIVITIES AT MPI HAMBURG*

L BENGTSSON AND L DÜMENIL
Max-Planck-Institut für Meteorologie, Bundesstrabe 55,20146 *Hamburg, F.R.G.*

(*Received* 18 *January* 1994; *Accepted* 31 *January* 1994)

Introduction

The third scientific group at the Max-Planck-Institute for Meteorology was established on 1 January 1991. It was successively built up during 1991 and in addition to the Director it consists of 6 scientists and 6 support staff. The group works closely together with the Climate Modelling Support Group set up by the German Climate Computing Centre (DKRZ) and the group of Klaus Hasselmann at MPI which focuses on the development and validation of coupled ocean/atmosphere models.

The methodology of the research is mainly directed towards the use of large scale comprehensive climate models and a considerable part of the work of the group is devoted to the development of an advanced atmosphere general circulation model (AGCM) including sub-models for land-surface processes and biomes.

The MPI meteorological climate modelling group has the following main scientific objectives:

- To further the physical and dynamical understanding of natural and forced fluctuations in the climate system with emphasis on the timescale 10^{-1}-10^{2} years. This research has the overall aim to obtain a more in depth knowledge of the effect of increasing greenhouse gases on the elimate system.
- To explore the predictability of coupled ocean-atmosphere systems.
- To undertake climate simulation studies, with the objective to identify the regional climate effects (Europe, North Atlantic region) due to the increase in the atmospheric concentration of greenhouse gases and other external forcing of the climate system.

In a joint effort, work is under way to evaluate the capability of El-Niño type predictions by a coupled ocean/atmosphere model. Work is also in progress to incorporate chemical processes with emphasis on the sulphur, methane- and ozone cycle.

Atmospheric Model Development

A major effort by the group has been the development of a global general circulation model, ECHAM3, which has been used for most of the numerical experimentation work during the period. ECHAM3 is based on the ECMWF 19-level spectral-transform model but has in several respects a modified physi-

*Belongs to Section I. Late receipt, hence added at the end of the volume.

cal parameterization, in particular concerning the handling of cloud- and radiation processes. Cloud water, for example, is handled as a separate 3-dimensional variable. A detailed description can be found in Roeckner *et al.*[1] and an up-to-date model documentation is available from DKRZ.

ECHAM3 has been developed and programmed in a flexible way and has been used in long-term integrations in T21, T42, T63 and T106 horizontal resolution. It has also been used in multi-year ocean-atmosphere coupled experiments.

Parallel to the experimentation with ECHAM3, a new AGCM, ECHAM4, has been developed and test integrations are in progress. ECHAM4 has a new radiation parameterization including the effect of the "exotic" greenhouse gases, CH_4, NO_2, CFC etc. Boundary layer processes are handled by a higher order turbulence closure parameterization and the advection of moisture and liquid water are treated by a semi-Lagrangian integration. An arbitrary number of tracers can also be handled by the semi-Lagrangian scheme (see 'Global Transport Modelling' on p. 436). The model can be extended to at least the stratopause using a uniform radiation code.

Experiments have been undertaken with a full semi-Lagrangian integration, but so far mass-conservation has been unsatisfactory when integrated over longer time-periods. A new long term experiment is in progress using a T63 resolution; this integration is expected to be available within a month or so.

For the study of regional processes, a high resolution, limited are grid point model, originally developed for short-range weather prediction in the Nordic countries, has been modified for climate research. This has been achieved by inserting the physical parameterization of ECHAM3 and increasing the number of vertical levels to be the same as in ECHAM3. The new model, HIRHAM, has been coupled to ECHAM and numerical experiments are in progress. HIRHAM is also programmed in a flexible way and can be used for arbitrary areas of the earth and for resolutions down to 10-15 km. HIRHAM will also be used in parameterization studies. Areas under consideration are Indonesia and Antarctica.

Work is also in progress to couple a non-hydrostatic model, GESIMA, developed at GKSS, Geesthacht, to HIRHAM and thus to obtain a series of atmospheric models from global scale down to the kilometerscale.

The model development work takes place in close co-operation with other German groups as well as groups in Europe and United States.

Modelling Research

Dynamical Regionalization

General circulation models are the main tools available today for climate change simulations. However, for the very long integrations of 100 years or so normally required in climate applications, models can only be run at relatively low horizontal resolutions. Although a doubling of the resolution used so far may be possible within the next few years, it is still too coarse to adequately

describe the regional climate details, required for climate change impact studies. Higher resolution simulations for time slices of the order of 10 years are possible and have been undertaken. Still higher resolutions down to 50km or less, however, can be reached by nesting a high resolution limited area model (LAM), covering a particular area of interest, into a course resolution global model. To pursue the latter possibility, a LAM, suitable for climate simulations has been developed in close cooperation with DMI and KNMI, the Danish and Dutch meteorological Services. This LAM, called HIRHAM, was developed by combining the physical parameterization package from the climate model ECHAM with the Nordic, Dutch, Irish operational forecasting model, which is called HIRLAM (High Resolution Limited Area Model). In close cooperation with DMI, the HIRHAM will be used in a series of experiments aiming at a verification of the nesting LAM-GCM technique for high resolution present day climate simulations over Europe. It is planned to test also a coupled atmospheric-oceanic LAM obtained by coupling HIRHAM with a limited area version of the OPYC ocean model.

These experiments which are part of an international project called "Regionalization" supported by the CEC and coordinated by B. Machenhauer, were started at MPI in January 1993. Several other projects in which HIRHAM might be used are presently under consideration. The increased resolution obtained with HIRHAM using a grid length of about 50km compared with the driving T42 ECHAM3 is illustrated in Figs. 1 and 2. The figures show for each model its orography and a 6 hour accumulated precipitation field. The corresponding synoptic situation as simulated by HIRHAM is illustrated by the surface map Fig. 3.

Design of a New Semi-Lagrangian Scheme

For short and medium range weather forecasting a shift from Eulerian to semi-Lagrangian integration techniques has taken place at several forecasting centres. The main reason for this development has been the increased computational efficiency of semi-Lagrangian models, but also an increased accuracy in the calculation of advection terms.

Due to problems with mass conservation in present semi-Langrangian models, climate modellers have so far hesitated to use these models, although increased resolution could be obtained for the same cost. Artificial corrections can be made each time step which prevents a systematic loss of mass during long integrations. Such corrections are, however, unsatisfactory, at least theoretically, as the mass which is added each timestep is evenly distributed over the globe and not added at the right geographical positions. Furthermore other important conservation properties of the continuous meteorological equations are not formally fulfilled in the present semi-Lagrangian formulations. How serious this is for long climate simulations is not known at present.

In order to assure an exact fulfilment of the most important integral constraints in the basic equations a new semi-Lagrangian formulation has been worked out. The idea is to use as prognostic equations Lagrangian forms of the continuity equation, the thermodynamic equation, the total energy equation and the angular momentum equation. These equations are discretized for vo-

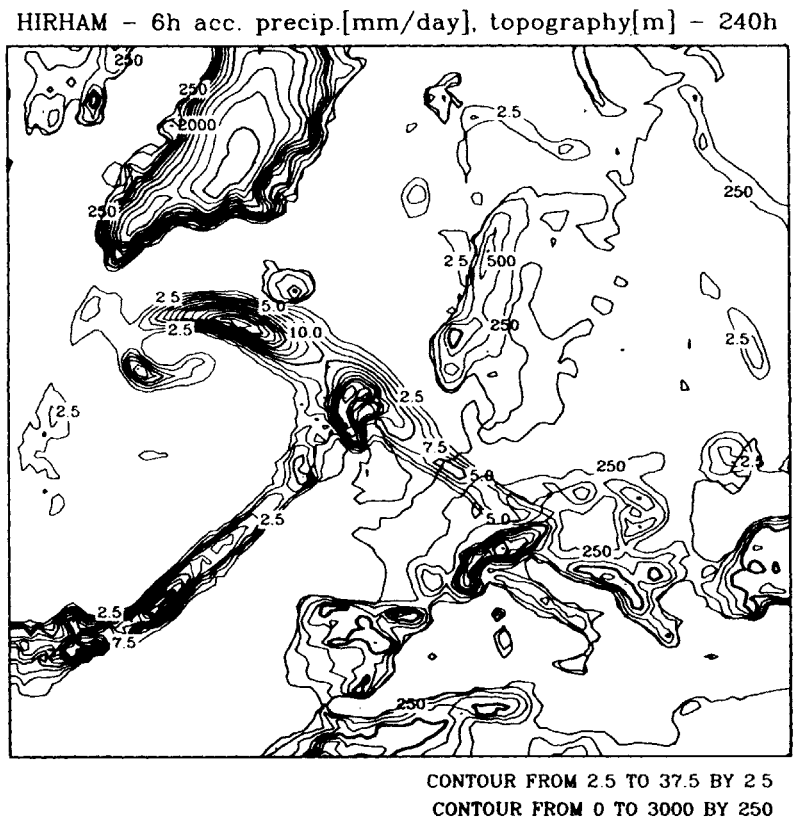

Fig 1 HIRHAM topography and 6 h accumulated precipitation. Contour lines for orography, every 250 m, and for precipitation, every 2.5 mm.

lumes of air that are being advected in the horizontal wind field at time t and are ending up after each time step (at time $t+\Delta t$) in the grid volumes. The continuity equation is used to define the top and bottom pressure of each air volume at $t\Delta t$ and t. The explicit leap frog time extrapolation scheme chosen must be absolutely stable since the total mass, entropy, energy and angular momentum are conserved (except for external processes) over each time step. This formulation will be tested at first for simplified geometries (1-D and 2-D) using the shallow water equations.

To test whether present semi-Langrangian formulations with mass corrections can be used for climate simulations, a comparison of three pairs of 5 years runs, each with an Eulerian and a semi-Langrangian model, is presently being done. These runs will be made with the ECMWF, NCAR and the Canadian (RPN) models.

Stratospheric Modelling

The aim is to construct a comprehensive model of the general circulation, of the troposphere and stratosphere with a uniform physical parameterization. The starting point is the ECHAM4 general circulation model which uses semi-

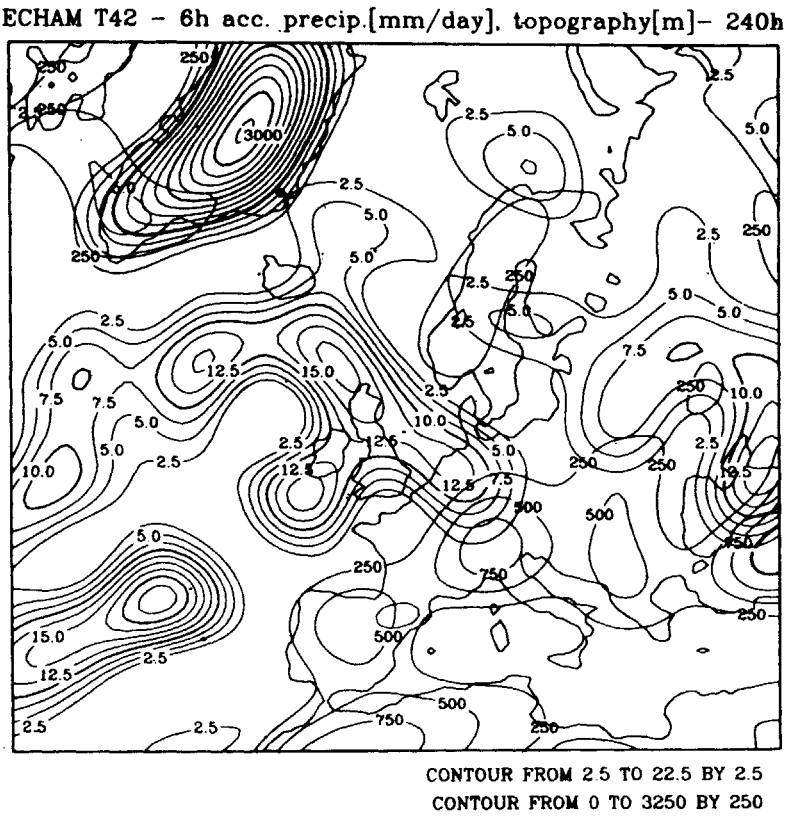

Fig 2 The same as Fig 1 but for ECHAM3 at T42 horizontal resolution.

Langrangian transport of water vapour and liquid water and a new radiation scheme.

The original ECHAM4 model has 19 vertical levels (hybrid vertical coordinate) with the top full-level pressure at 10 hPa (about 32km). A new vertical discretization was therefore necessary. In order to incorporate the whole stratosphere for such purpose an algorithm that generates vertical structures of the vertical coordinate has been constructed. This new algorithm allows a smooth increase of the spacing between adjacent vertical levels. Among the various vertical discretizations possible the following two have been selected: L25, with 25 vertical levels and top full-level pressure at 0.3 hPa (about 57km); and L35, with 35 vertical levels and top full-level pressure at 0.1 hPa (about 65km). In the upper troposphere and lower stratosphere L25 has the same vertical resolution of L19, while L35 has finer resolution than L19.

In constructing the new comprehensive model the physical parameterization has been uniformly extended through the stratosphere. However, it has been found that the approximate method to compute the longwave radiative heating rates in between full radiation time steps used in ECHAM3 fails in the upper stratosphere. This problem has been solved keeping the net longwave radiative flux constant between full radiation time steps. Since the standard full

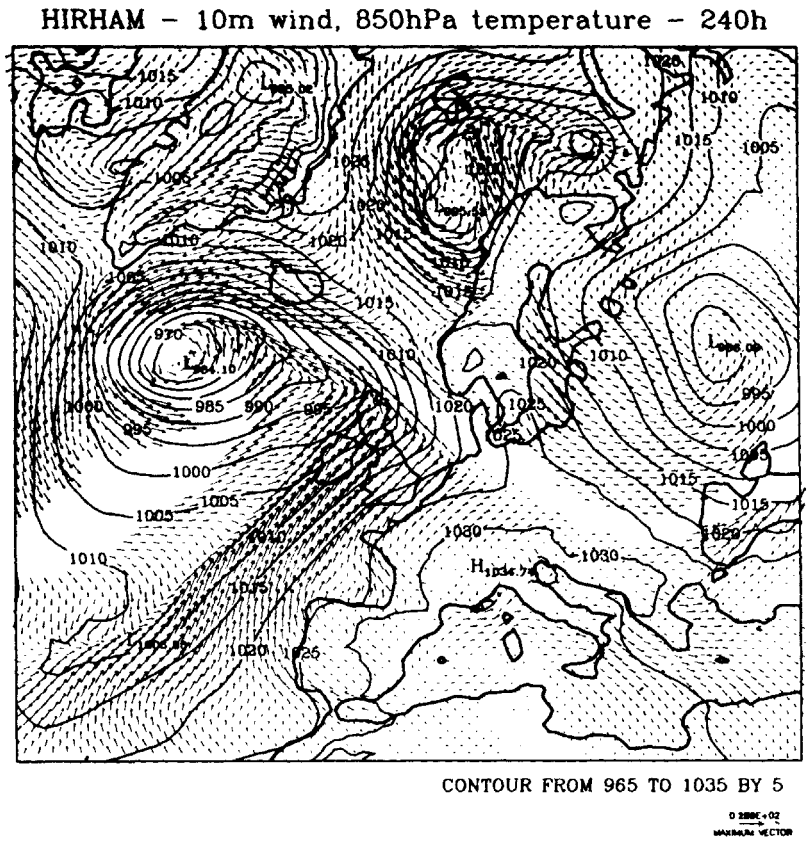

Fig 3 HIRHAM simulated wind at 10 m and temperatures at 850 mb. Colour changes for every 4°C.

radiation time step is two hours only, it appears acceptable to neglect long-wave flux variations over this time-interval. Without any other basic modification of the parameterization scheme, three integrations of the ECHAM4 model with L19, L25 and L35 levels respectively have been performed. Each integration has been carried out for 360 days with annual mean forcing (i.e. constant solar radiation, prescribed sea surface temperature and ozone distribution) and T21 spectral truncation. As initial state an isothermal, motionless and dry atmosphere has been used. Although some improvement is noted in the representation of the lower stratosphere (weakening and euqatorward shift of the stratospheric westerly jets), the results show the necessity of a revision of the radiation scheme above 10 hPa. Such a modification has now been done including the incorporation of the Voigt band correction.

Boundary Layer Investigations

Research on *scale aggregation over type-A landscapes*, i.e., terrain with changes in surface conditions at scales *smaller* than 10km, has focused on extending the so-called concept of blending height to include form drag due to roughness elements. Based on recent work, which indicates that small areas of

large roughness or minor obstacles dominate the regional momentum flux, whereas the regional heat and moisture fluxes are determined by the dominant surface cover, it has been hypothesized that regional momentum flux should be evaluated from an effective roughness length which implicitly accounts for the form drag of obstacles, whereas regional heat and moisture fluxes should be estimated from local surface parameters such as local roughness lengths. This hypothesis compares favourably with other, but less flexible, proposals when testing it in numerical simulations (Claussen 1992)[2].

The same hypothesis is applied when computing regional surface fluxes over partly forested areas. Here, neglect of air flow into and from the edges of tall vegetation appears to result in underestimation of local advection. On a regional scale, this 'edge effect' leads to an increase of momentum flux, but a decrease of latent heat flux (Claussen and Klaassen, 1992)[3].

The concept of blending height has been used to estimate atmospheric forcing in a large-scale sea-ice-oceanic mixed-layer model around Antarctica. The atmospheric drag on sea ice is computed from an effective roughness length which implicitly takes into account skin friction on ice and water as well as form drag on ice floe edges. Furthermore, the atmospheric drag depends on regional thermal stability. It turns out that, particularly in the Wedell and Ross Seas, an upward heat flux is diagnosed, although the atmospheric surface layer is stably stratified at the regional scale—an illustrative example of the so-called Schmidt's paradox. The new parameterization leads to improved model results in terms of ice-thickness distribution, ice velocities, mixed-layer depth and mean oceanic heat flux (Stössel and Claussen, 1992)[4].

Research on *scale aggregation over type-B landscapes*, i.e. terrain with variation in surface characteristics at scales *larger* than 10km, is in progress. It seems that some ideas valid for scale aggregation at small scales can simply be extended to larger scales. Although further testing has to be done, a simple version has been tested in ECHAM3. First results show that horizontal gradients of near-surface temperatures at the east coasts of continents during winter are smoothed leading to less extreme changes in heat fluxes. Morevoer, the monthly mean isotherms of near-surface temperatures look more realistic than in the original model, where, in many cases, they simply follow the coarse land-sea mask.

Cloud-Radiation Processes and Their Implication on Climate

In ECHAM, stratiform clouds are simulated on the basis of a cloud water transport equation including sources and sinks due to condensation, evaporation and precipitation formation by coalescence of cloud droplets and sedimentation of ice crystals. The predicted cloud water content is used to parameterize the cloud optical properties such as emissivity and optical depth.

Satellite data of the Earth Radiation Budget Experiment (ERBE) are used to validate the model simulations, in particular the cloud radiative forcing (CRF) which is the contribution of clouds to the shortwave cooling and longwave warming, obtained by subtracting the respective clear-sky estimate from the total. According to Fig. 4-a-c, there is generally good agreement between

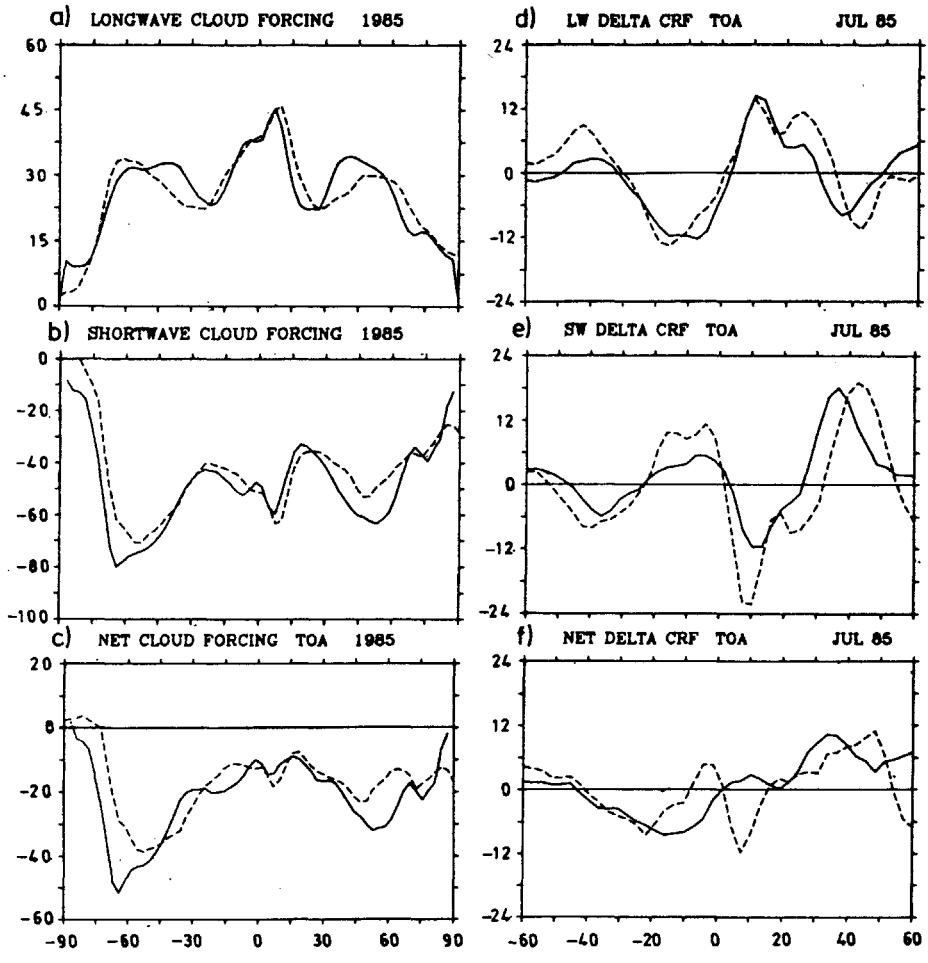

Fig 4a-f Annual zonal mean cloud forcing (Wm^{-2}) as analysed from ERBE data (full lines) and as simulated by ECHAM3-T42 (dashed). (a-c)
Response of the cloud forcing (Wm^{-2}) to seasonal thermal forcing for July 1985, as analysed from ERBE data (full) and as simulated by ECHAM3-T42 (dashed). Positive values correspond to a warming relative to the annual mean and negative values correspond to a cooling. (d-f)

the simulated (ECHAM3-T42) and observed CRF for 1985 (the model is forced with the respective SST for that particular year), and the deviations are mostly within the range of observational error which is around 10 W/m^2 for zonal means. On the regional scale (not shown) the deviations are larger and more significant. For example, the shortwave CRF is overestimated in areas of persistent tropical convection and underestimated over the northern oceans during the summer season due to a lack of low-level cloudiness.

Satellite data can also be used to validate cloud variations resulting from observable forcing such as the seasonal or ENSO cycles. As an example, Fig. 4d-f compares the observed and simulated CRF response to seasonal thermal forcing (July 1985 vs. annual mean 1985). Both, model simulation and ERBE

data indicate a net mid-latitudinal warming of the summer hemisphere with respect to the annual mean (i.e., an amplification of the seasonal warming by the change of cloudiness), caused by a reduced shortwave CRF as a result of the seasonal transition of cloudiness over the Northern Hemisphere continents from a stratiform regime in winter to a convective regime in summer. In the tropics, the change of the cloud forcing (both components) is just a response to the seasonal shift of the ITCZ. While the model is able to reproduce the observed CRF response with some success, there is clearly an overestimation of the shortwave response in the tropics. Accordingly, the sign of the net response is reversed (damping of the seasonal wave instead of a slight amplification as suggested by the ERBE data). However, these preliminary results should be taken with caution because interannual variability and observational errors have to be considered as well.

It is well known that the atmospheric circulation in the tropics is largely driven by the release of latent heat in deep convective towers. On the other hand, very little is known about the radiative impact of these clouds on both the atmospheric circulation and the oceanic heating. In a collaborative effort together with the SCRIPPS Institution of Oceanography (Professor V. Ramanathan) a series of model experiments has been designed in order to study the interaction between cloud-radiative effects and the tropical circulation. Preliminary results obtained from this ongoing work (which will gain observational support from the CEPEX experiment in the tropical Pacific during March 1993 as well as TOGA-COARE) may be summarized as follows:

- In areas of persistent convection, as for example over the warm pool in the West Pacific, the net radiative heating by clouds (i.e. the atmospheric contribution to the cloud radiative forcing) contributes 20-30% to the total diabatic heating.
- Most of the radiative heating is provided by the trapping of upwelling infrared radiation by optically thick cirrus anvils above 400 hPa.
- Neglecting the radiative heating by the cirrus anvils causes a substantial weakening of the tropical circulation (Hadley and Walker cells), see Fig. 5.
- The most sensitive area in this respect is the warm pool area in the West Pacific.

According to Houghton *et al.* (1990), the current estimates of the equilibrium temperature response to a doubling of CO_2 range between approximately 3 and 5°C in the global annual mean. Most of these uncertainties are attributed to different climate sensitivities of the models, caused primarily by large differences in the simulated cloud feedbacks. A recent model intercomparison study initiated by Professor R.D. Cess aimed at comparing the $2 \times CO_2$ forcing rather than the climate feed-backs and suggests that a sizeable fraction of the simulated temperature range (up to 50%) may be explained by the different radiative forcing. The CO_2 forcing problem has been addressed in a joint effort among 14 GCM groups (including MPI). For computational reasons the models are run in a perpetual July mode. The radiative transfer code is called 4 times during a time step (pair of $1 \times CO_2$ and $2 \times CO_2$, with and without clouds respectively). In this simulation 3 of the 4 heating rate calculations are

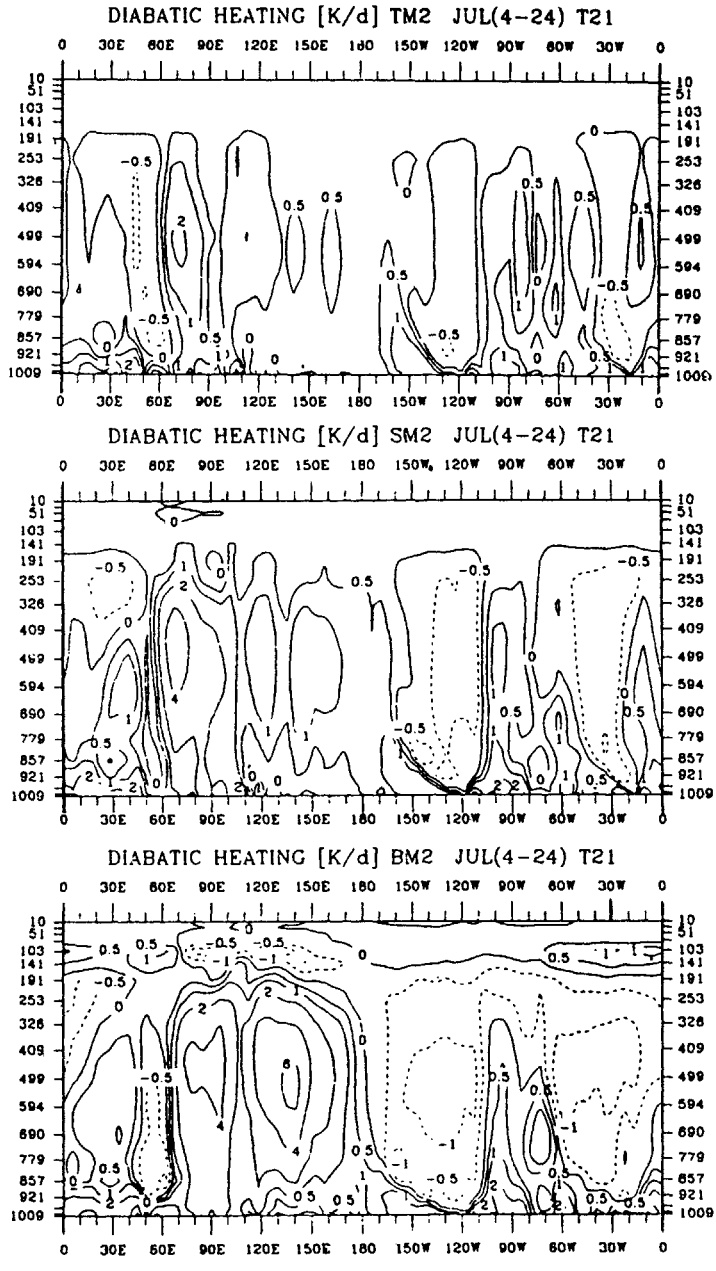

Fig 5 Longitude (0-30°N)/height (pressure).
Cross sections of total diabatic heating and velocity potential as obtained from three 24-month perpetual July simulations with the ECHAM3-T21 model with different assumptions on cirrus cloud emissivity:

(Continued on page 417)

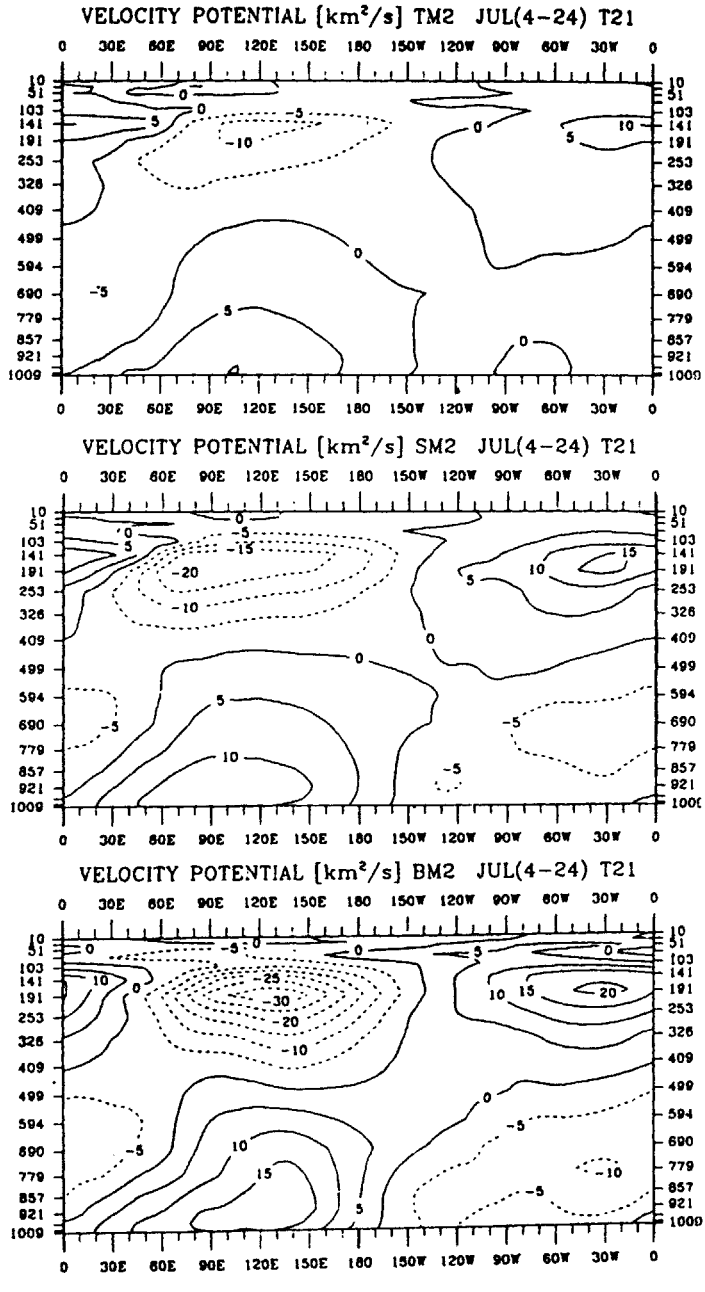

(Fig.5 contd.)

Top:	Transparent cirrus in the infrared
Middle:	Variable cirrus emissivity depending on cloud water content (Control experiment)
Bottom:	Black cirrus

just performed to diagnose the forcing without changing the model climate. Additional column experiments are performed for mid-latitude summer conditions and the results are compared with exact line-by-line integrations. The main conclusions from this intercomparison study are:

- The range of uncertainty is about 30% of the mean tropospheric forcing which is close to 4 w/m^2. Most of this uncertainty comes from the different treatment of the CO_2 absorption bands in the various models. Overlap effects due to water vapour and clouds and solar absorption do not contribute tot he variations in the forcing estimates.
- As compared to line-by-line models, the broad-band radiative transfer codes used in the 14 GCMs tend to underestimate the longwave $2 \times CO_2$ forcing (mid-latitude summer, clear sky). Part of this underestimation is due to the neglect of certain CO_2 absorption bands in the broad-band models.

Development of Rainfall Run-off Scheme

In order to allow a meaningful estimate of the continental runoff which is used as fresh water input into the ocean in coupled ocean/atmosphere integrations, a rainfall/runoff scheme (Dümenil and Todini, 1992)[5] and a river routing scheme (Sausen, Schubert and Dümenil, 1992)[6] were developed. The rainfall/runoff component is a simplification of a state-of-the-art approach which is employed in hydrological modelling. The scheme takes into account the heterogeneity of the land surface within a grid area. It is the first application of such a model in a GCM. It is combined with a global data set on soil water holding capacities. The model is being intercompared together with more sophisticated hydrological models currently being used in other GCMs in the framework of the EC project on Spatial Variability.

The Global Runoff Data Centre (GRDC) has been approached with a request to provide data from their archives for model validation. At a first instance, longtime series of measurements for the 10 largest rivers of the world was selected. This has now been extended to include the 50 largest rivers (Dümenil *et al.*, 1993)[7]. Time series and long-term averages of monthly means are now available. The data provide an independent and valuable data set for validation of the hydrological cycle in the model. Model verification for individual basins is in progress.

Validation Studies

Results from several 10-year integrations with and without observed sea surface temperature, SST, have been investigated with respect to systematic deviations of the model runs from reality. These investigations cover a wide range of studies including the validation of:

(i) the large scale dynamic circulation;
(ii) the interannual variability;
(iii) regional climates;
(iv) physical processes including certain aspects of the hydrological cycle; and

(v) phenomenological evaluations such as blocking, extra-tropical cyclone tracks, tropical cyclones etc.

Some result of this work is reported in Roeckner *et al.* (1992)[1]. Several other aspects of the validation of ECHAM3 is presently being written up and hence only a summary of this work will be reported here.

Large Scale Systematic Errors

The monthly averaged or seasonally averaged circulation agrees well with observations except in a few areas. For the Nothern Hemisphere winter the following could be mentioned:

(i) The Atlantic subtropical anticyclone has a more easterly position and the Azore high has a centre over Spain. In connection to this the east Mediterranean trough is too weak.

(ii) The Aleutian low is positioned too far eastwards and is also too confined in the north-south direction.

(iii) The trough over the western Pacific and the ridge over Alaska at 500mb is too weak.

However in making these remarks, it should be noted that at several winters such features are actually observed in nature the only difference is that they appear more often in the model calculations.

The high as well as the low frequency variability is realistic, Fig. 6, although there exist a slight tendency to underestimate low frequency variability and overestimate high frequency variability.

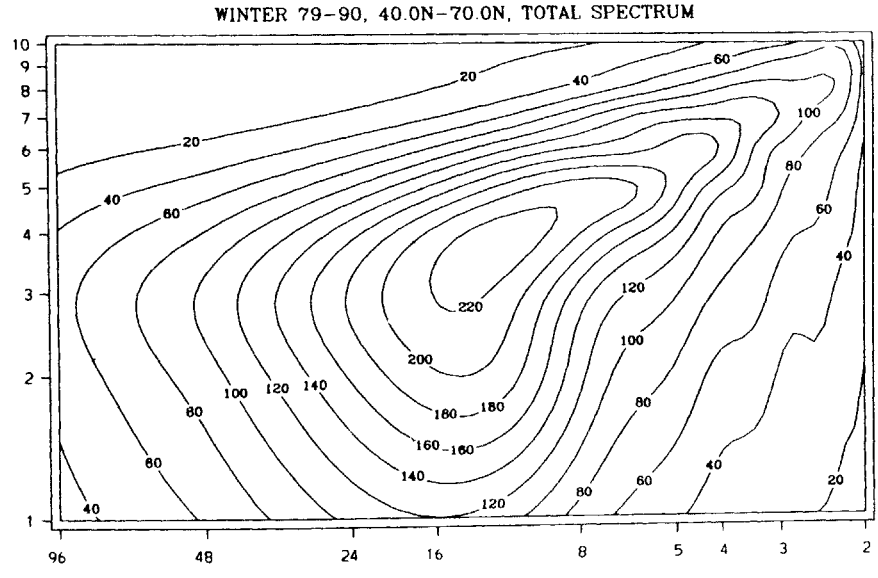

Fig 6(a) Power spectrum of geopotential at 500 hPa and 40° N-70° N for winter derived from 12 years of ECMWF analysis. Units are 100 m^2, on the abscisa the period (days) and on the ordinate the zonal wavenumber are given both in logarithmic scale. The spectral estimates were multiplied by wavenumber and frequency. Winter was defined as a period of 96 days starting December 1.

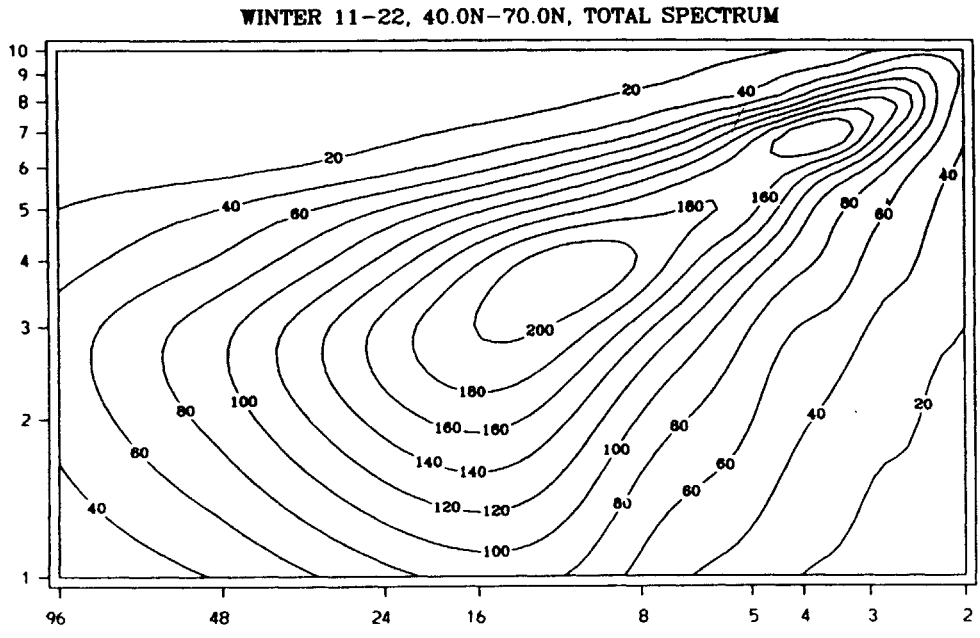

(b) The same as 6a but for 12 years of an ECHAM3 experiment using observed SST.

The interannual variability at middle and high latitudes agrees well with ECMWF's analyses the effect of observed SST's in the Tropics describes more than 50% of the variance, but hardly any effect at all can be found in extra-tropics. See further 'SST-Impart Studies' that follows later.

The overall climatology of the simulations has been studied in its regional details. This has been accomplished by expressing the results of the simulations in terms of Köppens classification (Lohmann *et al.* 1992)[8] and also to calculate what biomes the model simulates. (*vide* also section on 'MONEG-Experimentation').

Such validation do efficiently highlight specific model deficiencies of particular importance for climate impact studies examples are too high precipitation over Australia and South Africa during the Southern Hemisphere summer. Over the Northern Hemisphere there is a tendency to simulate too little precipitation over land during the summer and in some areas, like the central part of United States the surface temperature in summer is also too high. As is being discussed below it is not clear to what extent this is caused by the handling of land-surface processes or whether the problems are related to deficiencies in the large scale circulation such as dynamical forcing caused by a too high precipitation over central America (in all likelihood due to orographic representation difficulties at T42 resolution).

Low Frequency Variability

In order to distinguish processes influencing the atmospheric variability by spatial and temporal scales a space-time spectral analysis was performed. As a result the spectral distribution of both stationary and transient eddies was

given. It is found that the "ultralong" transient waves (zonal wavenumber 1 to 3) give major contributions in the time range longer than 10 days, whereas those with a shorter wavelength (zonal wavenumber 4 to 7) have their maximum at periods shorter than 10 days.

As a consequence the data were subjected to a low- and a band-pass filter, the first one retaining eddies on time scales beyond 10 days, the latter one between 2 and 10 days. Thus we could distinguish the part of the atmospheric variability resulting from low-frequency and higher frequency disturbances. Another band-pass filter retaining eddies on time scales between 2 and 6 days, commonly used in many studies, was also applied to the data. Both band-pass filters lead to similar spatial structures, the 2-to-10 day filter, however, had significantly higher variance.

The distinction between the low- and higher frequency eddies as described above was also considered in the localized "Eliassen-Palm Flux" diagnostics. Thus we could investigate the impact of the transient eddies on the zonal mean flow. Those, for example, are thought to play an important role in initiating and maintaining a "blocked" flow and other quasi-stationary features.

As a prominent example of a low-frequency phenomenon blocking was investigated. Based on different theoretical descriptions various criteria were applied in order to identify episodes, when a blocked flow occurs in the extratropics region. It seemed that the criterion based on the "persistence" of such a phenomenon was the most appropriate one for our purposes, in particular as it can be applied on both hemispheres, but can also be used to identify other low-frequency phenomena in the extratropics such as "Cut-off Lows".

As a result individual episodes of Blocking were defined for particular locations leading to frequency distributions of this phenomenon distinguishing by seasons. Some of these episodes, however, will also be subjected to more detailed diagnostics considering important physical processes leading to a blocking flow regime.

As was seen from the spectral analysis the ultralong westward travelling waves give a major contribution to the atmospheric variability in the time range beyond 10 days. For that reason a first attempt was made to investigate a possible relation between the activity of these waves and the occurrence of blocking.

The Hydrological Cycle in the ECHAM3 Model

The group is spending considerable efforts in validating the hydrological cycle. Comparison with different climatological estimates show good agreement and in fact in many respect the different climate estimates differ between themselves as much as to the models results. Fig. 7 shows the estimated and simulated hydrological cycle for the Earth. Fig. 8 shows the same for the zonally averaged precipitation summer and winter respectively. Intercomparisons have also been undertaken against satellite estimates from OLR and SSM/I measurements as well as against land station data compiled and analysed by GPCC (Global Precipitation Climatological Centre) in Offenbach. GPCC has made data available for 1987 and 1988. These data have been compared with model integrations for the same period (using observed SST data).

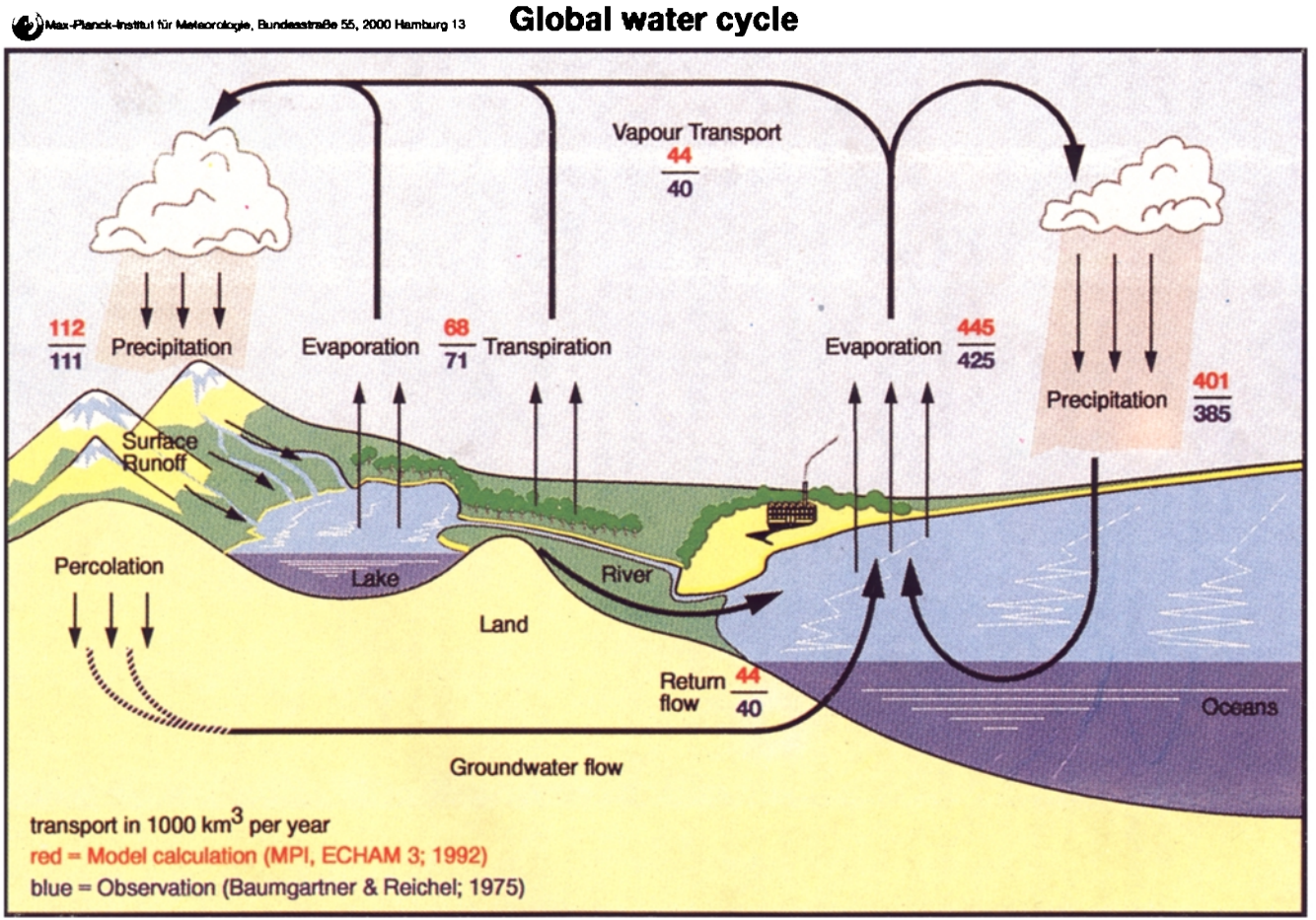

Fig 7 The annual global water cycle calculated from ECHAM3-T42 averaged over 10 years (upper figure). Evaporation and precipitation are calculated, atmospheric water transport and river return flows are obtained as residuals. Unit 1000 km^3/year.

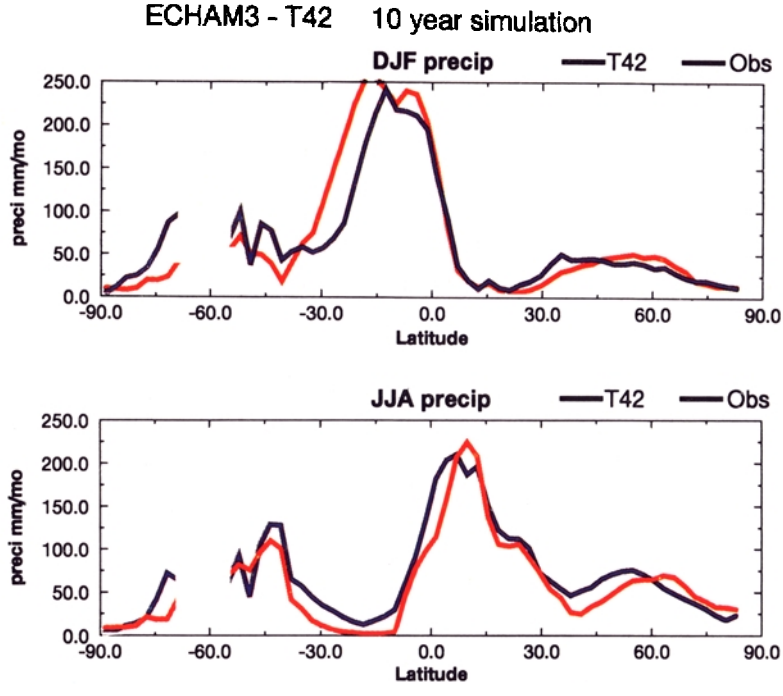

Fig 8 Precipitation over land for winter and summer respectively. Thin curve ECHAM3-T42, heavy curve climate estimate.

The agreement with the GPCC data is generally good, although the regional precipitation difficulties discussed above can also be seen from the GPCC data. There are considerable differences between the GPCC data and OLR data over land and between OLR data and SSM/I data over the oceans stressing the serious problem with the validation of precipitation.

Work is also under way to use river run-off data as an additional way to validate the hydrological cycle. A few such areas have already been investigated highlighting several interesting aspects.

For the Amazon catchment area the model is simulating the annual cycle of precipitation reasonably well, perhaps with a slightly too large amplitude. During June/July/August the precipitation amounts are very low both in reality and in the simulations but due to insufficient storage of water in the ground or in the river area in the model calculations these low precipitation rates lead to unrealistic drying of the ground with reduced evaporation and too high simulated surface temperatures.

When comparing with river runoff data from the model with observed ones for subarctic regions, for example, the MacKenzie river or the river Ob, one finds unrealistic strong runoffs during summer time. This is related to an overly high accumulation of snow especially during the spring. Where observations already show melting of snow in spring one still finds an accumulation of snow in the simulations. It is believed that the ageing of snow should lead to a reduction of the albedo. Over rough ground one would expect snow free

areas which would as well lead to reductions of the albedo in snow situations. Both effects are not accounted for in the present parameterization scheme but could at least partly reduce the too late melting of snow in the area.

Land-surface Proceses

One systematic error common to several GCMs is the erroneously strong warming of the near-surface atmosphere in the Central United States in the summer. Also in the ECHAM3 model simulation too little precipitation occurs in this region, Fig. 9, and as there is plenty of energy available for evaporation, the soil dries out in the course of the integration and subsequently warms up excessively during the summer. This is not observed.

A series of experiments has begun in order to clarify whether the errors in this area are due to errors in the large-scale dynamics or if they are related to the representation of the flux of moisture from the land surface. These experiments will assess the sensitivity of the annual cycle of precipitation to the specification of the properties of the soil moisture reservoir and the general formulation of the equations governing the evaporation from bare ground or through plants.

Fig. 9 shows the results from the T21 control integration, two T21 experiments with modified boundary conditions and a T42 control integration. The atmosphere is combined with an ideal boundary condition of soil moisture (from a climatology by Mintz and Serafini, 1981)[8a] in experiment CLIS and a saturated soil (which should satisfy the atmospheric demand at all times) in experiment SATS.

In the T21 model soil wetness during the year varies between 20 and 40%, while according to climate it is 80% during the winter and spring and 20% during the summer. The model produces rainfall of the same amount as is observed in summer, but less than observed during winter and spring. Con-

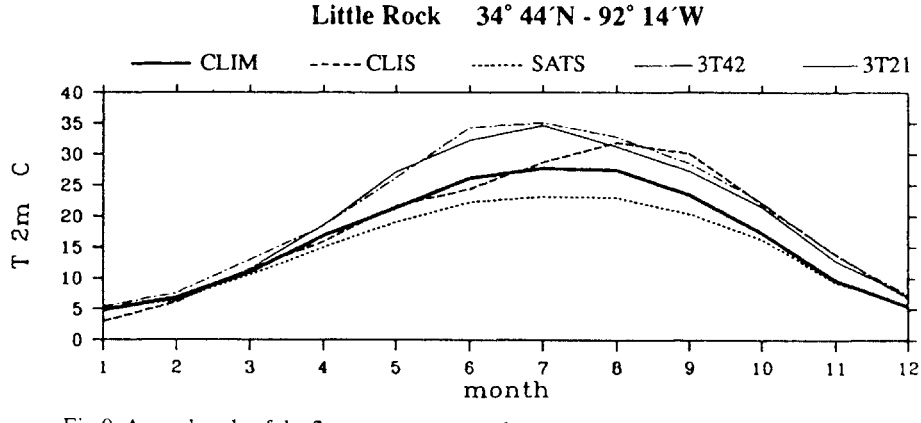

Fig 9 Annual cycle of the 2 m temperature at the model gridpoint nearest to Little Rock.
CLIM: climatology 1931-1960
3T21: from 20 years of integration with the ECHAM3 model at T21 resolution
3T42: as 3T21 but for doubled horizontal resolution.
CLIS: as 3T21 but using soil moisture boundary conditions from climatology
SATS: as 3T21 but using soil moisture boundary conditions at saturation.

sequently, the soil moisture reservoir in the model cannot be refilled which in turn is likely to suppress precipitation further. The error in the winter precipitation is both influenced by the surface boundary condition and the large-scale circulation. Precipitation increases if climate boundary conditions are applied, but is still not sufficient even if the soil is saturated. This suggests that even with correct boundary conditions the moisture transfer is not strong enough to enhance precipitation by local processes and hence, the problem is presumably related to moisture transport by the large scale circulation. This is suggested by the fact that precipitation is increased with higher horizontal resolution. Experimentation will be continued.

Low Frequency Analysis of Equatorial Zonal Wind

The dynamical properties of ECHAM3 have been verified by comparing the power spectrum of different model quantities with the corresponding analysed and observed power spectra.

Such a test was carried out for the zonal wind as observed at Singapore (Fig. 10). The "model" power spectrum was computed and averaged for two AMIP-simulations driven by the observed sea surface temperature of January 1979 to December 1988. The "analysis" power spectrum is based on ECMWF analysis data for January 1981 to December 1990. It is worthwhile to keep in mind that the analysis procedure has undergone some changes during this period. The power spectrum for these two cases was computed by a maximum entropy method using the Burg algorithm and 20 poles. These power spectra were compared with the "observation" power spectrum of the zonal wind at Singapore. The observations cover the years 1968 to 1985. The analysis is based on the same method but uses 40 poles.

Fig. 10 shows the power spectra of the zonal wind on 850mb, 200mb and 50mb, representing the dynamical behaviour near the surface, in the upper troposphere and near the top of the model. The comparison gives the following main results for the three levels:

(i) 850mb
The analyses contain only the annual cycle, while the model shows in agreement with the observed data, a low frequency peak (related to El Nino) as well. The semi-annual peak is hardly visible neither in the analysed data nor in the model simulation. (700hPa-spectra have the same characteristics).

(ii) 200mb
Analysis and model data show qualitatively the same spectrum: semi-annual and annual peak plus the multi-annual frequency variability. Differences are presumably also due to the short data base for the analysis and the model data.

(iii) 50mb
Analyses and observations contain a distinct quasi-biannual oscillation (QBO) signal while the model is not able to reproduce this phenomenon.

Although this test is incomplete since it only includes one particular station (power spectra for the model and the analysis have been calculated for the

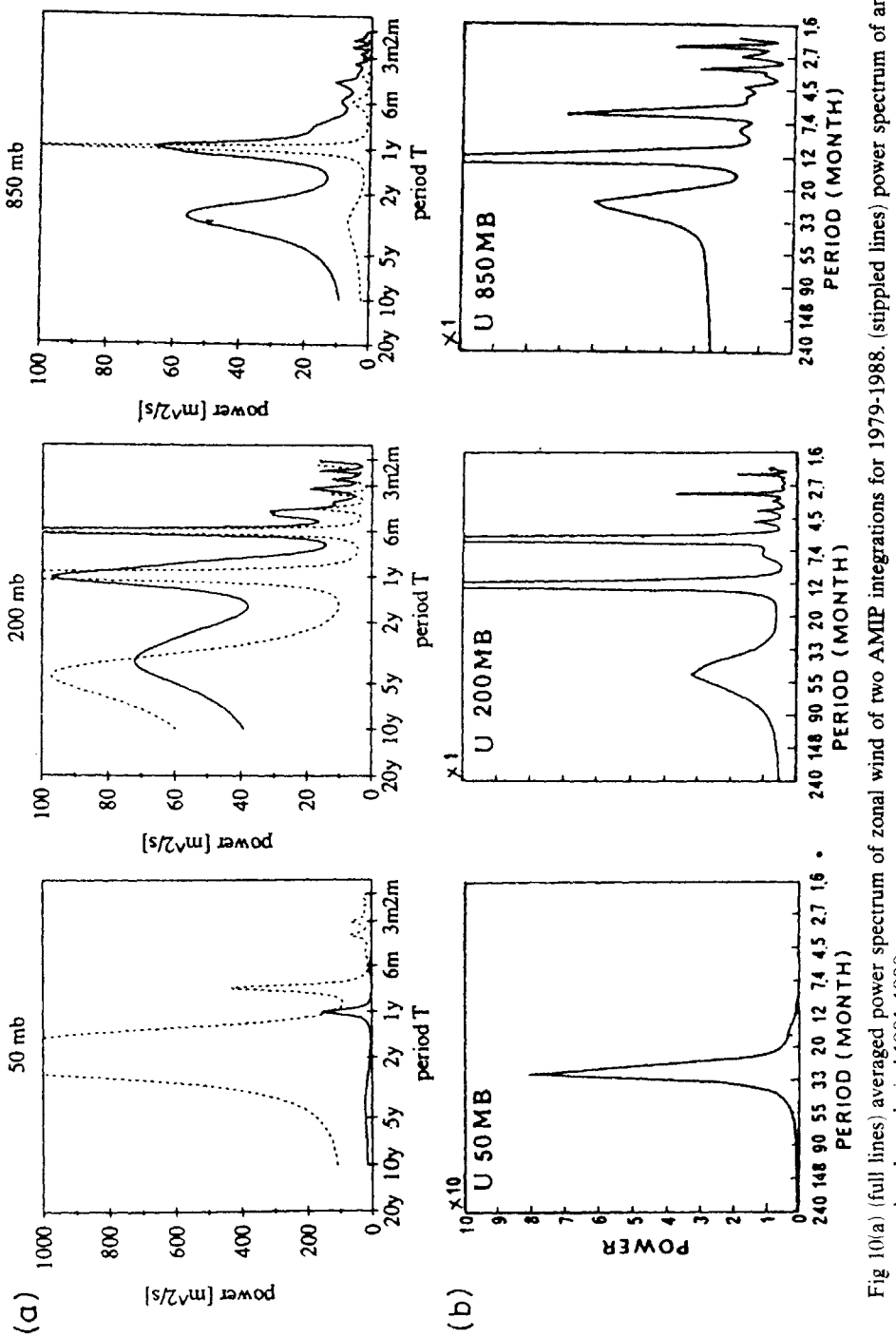

Fig 10(a) (full lines) averaged power spectrum of zonal wind of two AMIP integrations for 1979-1988. (stippled lines) power spectrum of analysed zonal wind 1981-1990.

(b) (full lines) spectrum of observed zonal wind according to Yasunari 1989 *J met Soc Japan* **67** 483-493.

whole equatorial domain) it shows that tropical *analysis data*, as they are available now, can show severe deviations from the dynamical behaviour of *observed data*. It is thus interesting to note that the ECHAM3 shows a multi-annual frequency variability of the tropospheric zonal wind above Singapore that agrees at least qualitatively with the observed variability. No QBO signal can be found in the model simulation.

SST-Impact Studies

The SST-anomalies during El Niño events have been found in several studies to be a major cause to anomalous circulation in the tropics. In order to make an in depth study of this forcing and to find out to what extent the ECHAM3 model could simulate it, a series of multi-year integrations using observed SST (1979-1991) and climatological SST (over the same period) have been undertaken with the following objectives:

(i) To explore the geographical distribution of the impact of SST-anomalies.
(ii) To investigate the reprodubility of this impact.
(iii) To investigate the role of El Niño SST anomalies and other tropical anomalies versus the anomalies in the North Atlantic.
(iv) What basic mechanism in the ocean/atmosphere system are responsible for the observed propagation of equatorial SST-anomalies from one ocean basin to another e.g. from the East Pacific to the Atlantic?

Preliminary results based upon an ensemble of four 10-year integrations, two using observed SST and two climatological SST, and a few additional shorter calculations for the 1982/83 event suggest the following.

There are considerable differences in the response between the tropics and extra-tropics. This can be seen in a more general way from Fig. 11 which shows the 500mb seasonal variability of JJA for the control run (using climate SSTs), the run with observed SSTs and the observed variance (from ECMWF analyses). Results from other seasons are similar. As can be seen the variance increased enforced by the observed SSTs is essentially more than doubled compared to the control run and is also in reasonably good agreement with observations.

Generally the El Nino events can be identified in all basic parameters in the tropics in particular in the upper air circulation. Precipitation anomalies are very well correlated with OLR (over oceans), and where available with *in situ* observations over land certain areas like the Sahel region and India is less good than other areas indicating more complex relation or model deficiencies. In the extra-tropics, Western Canada and United States are excellent and most major variables vary in phase with El-Niño. The signal of the European, on the other hand, is weak and here the inter-annual variability is strongly dominated by the chaotic internal variability.

The reproducibility of the result or lack of reproducibility support this result. This can be seen from Fig. 12 which shows the precipitation in two areas, central tropical Pacific and central Europe as simulated for two different runs starting from different initial conditions.

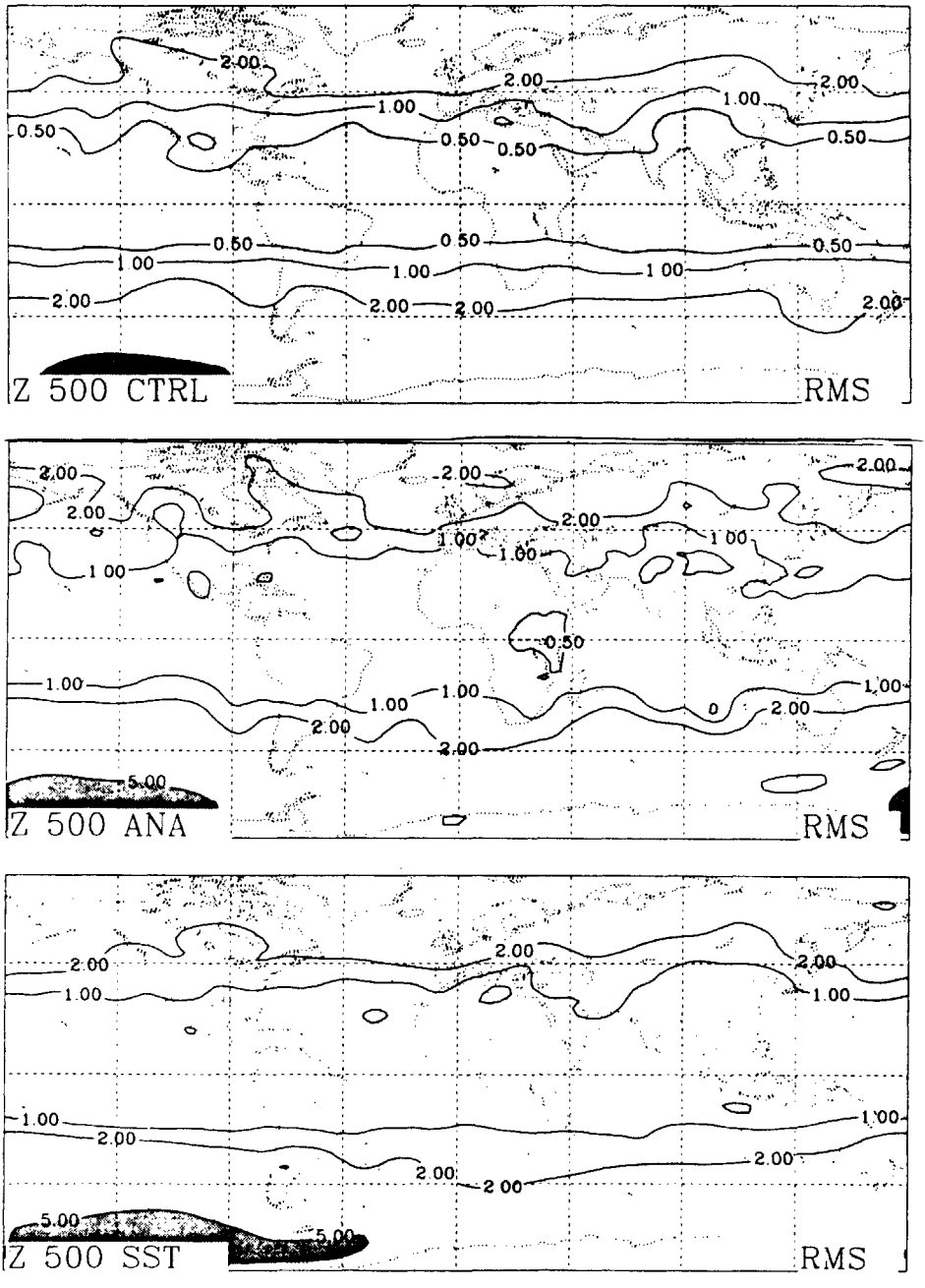

Fig 11 RMS variability in summer (JJA) at 500 mb of seasonal means 1979-1992. (a) shows the control experiment using climatological SST data (monthly averaged 1979-1992), (b) calculated from ECMWF analyses and (c) from the experiment using observed SST data.

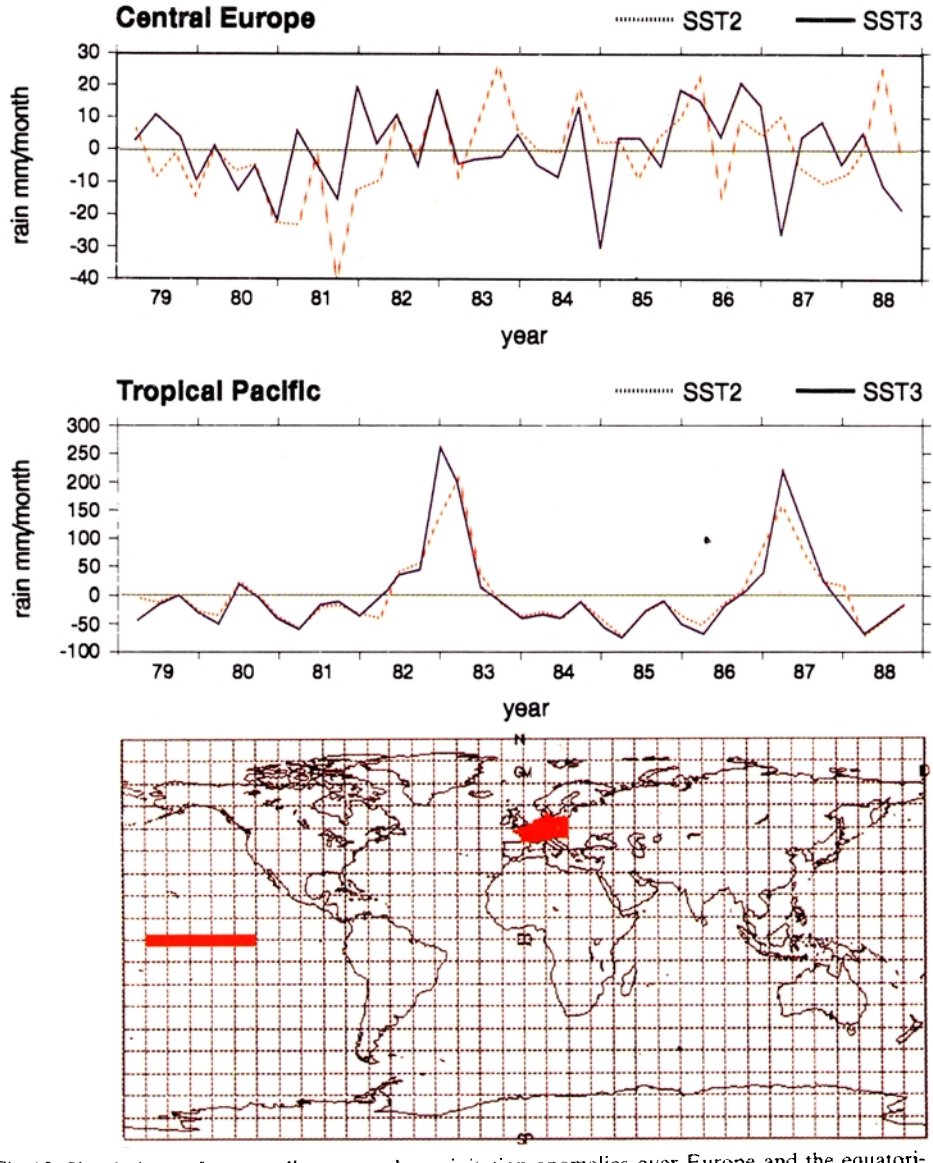

Fig 12 Simulations of seasonally-averaged precipitation anomalies over Europe and the equatorial eastern Pacific (see **lower panel**), obtained in two independent ten-year integrations with the ECHAM3 atmospheric circulation model. Observed sea-surface temperature and sea-ice conditions (as specified in the AMIP) were used in both integrations, but initial atmospheric conditions were different. Note the lack of a reliable climate signal in mid-latitudes (**upper panel**) and the high degree of reproducibility in the equatorial Pacific.

Attempts have been made to find a relation between North Atlantic SST anomalies during the period 1979-1992 and circulation anomalies. Any such relation of any meaningful amplitude has not yet been identified.

Longitude-time diagrams for tropical means of several variables show a slow eastward propagation in the experiments as well as in analysis data. The

period is round 5 years. In the 200mb U field anomaly this propagation is appearing to move around the world with unchanged amplitude while for most other variables (precipitation, OLR, vel. pot. at 850and 200mb) the features are starting over the Indian Ocean, increase in amplitude over the Pacific, with a strong reduction in amplitude over America and a fading away over the Atlantic. These features are more distinct and have larger amplitudes in the experiments but also evident in the observations. The investigation did concentrate on the period 1979 to 1992 with 3 El Niño events.

Another similar, very slow propagation but from the equator towards the poles has been found by Dickey *et al.* (1992)[9] for the angular momentum. This can also be seen in the experiments.

The investigation concentrated on the question if these apparent travelling waves are real propagations caused by an atmospheric mode or if the atmosphere passively reacts to SST anomalies which then appears like a travelling wave. Experiments with monthly mean climatological SST do not show such a propagation which suggests that the propagations in the atmosphere are only forced by the SST anomalies. Using atmospheric data from a climatological SST experiments and switching on observed SST anomalies establishes the propagating wave within a month. Also switching off the observed SST anomalies in a run during the most intense phase of El Niño lets the wave fade away within a month. So the atmosphere does not remember atmospheric anomalies for a long time and what we see therefore is in all likelihood a direct effect from the SST anomalies.

An experiment in which the atmosphere is only forced from the SST anomalies from the Pacific shows very similar propagations of a wave and similar atmospheric anomalies as the experiments with the complete SST anomalies which suggests that it is mainly the Pacific which gives a clear effect.

However, the atmospheric circulation is needed to propagate SST anomalies e.g., to allow SST anomalies to move over the American continent into the Atlantic. It can be explained by the anomalous atmospheric circulation during such events.

MONEG-Experimentation

The group has contributed to the design of the experimentation strategy of the TOGA Monsoon Experimentation group and has been actively involved in performing and diagnosing the proposed set of numerical experiments. The aim was to intercompare the skill of 16 global atmospheric models with regard to the interannual variability of the northern hemisphere summer monsoon. Concerning the causes of this variability, the following hypothesis were tested in 90 day integrations: The model's skill in representing this variability may be influenced either by boundary conditions such as sea surface temperature anomalies or anomalies in land surface conditions or by the initial state of the atmosphere. In the beginning of the project, the example of the years 1987 (poor Indian monsoon) and 1988 (abundant Indian monsoon) was studied in order to investigate the role of the sea surface temperature anomalies in individual ocean basins. The simulation using the ECHAM3 T42 model as well as

13(a)

13(b)

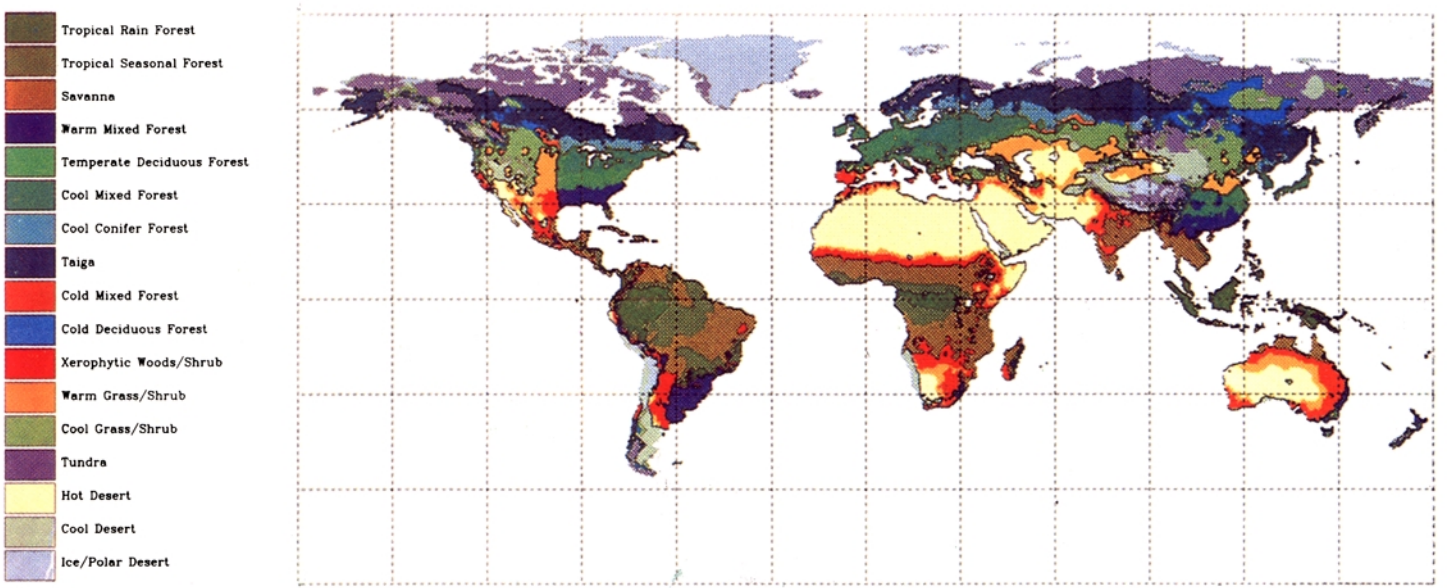

Fig. 13(a) Summary of biomes used and allocation of colour to the biomes depicted in the maps.

(b) Present natural biome distribution computed from observed climatology.

those of the models showed that in this particular year the monsoon variability was forced by a relatively large Pacific Ocean sea surface temperature anomaly, with a small counteracting influence by the small anomaly in the Indian Ocean (Dümenil and Roeckner, 1992)[10]. Experimentation was continued for anomalies in the level of soil moisture over the Eurasian continent. The impact of this anomaly taken from analysed soil moisture fields from ECMWF for 1987 and 1988 is only small. Experimentation will be continued.

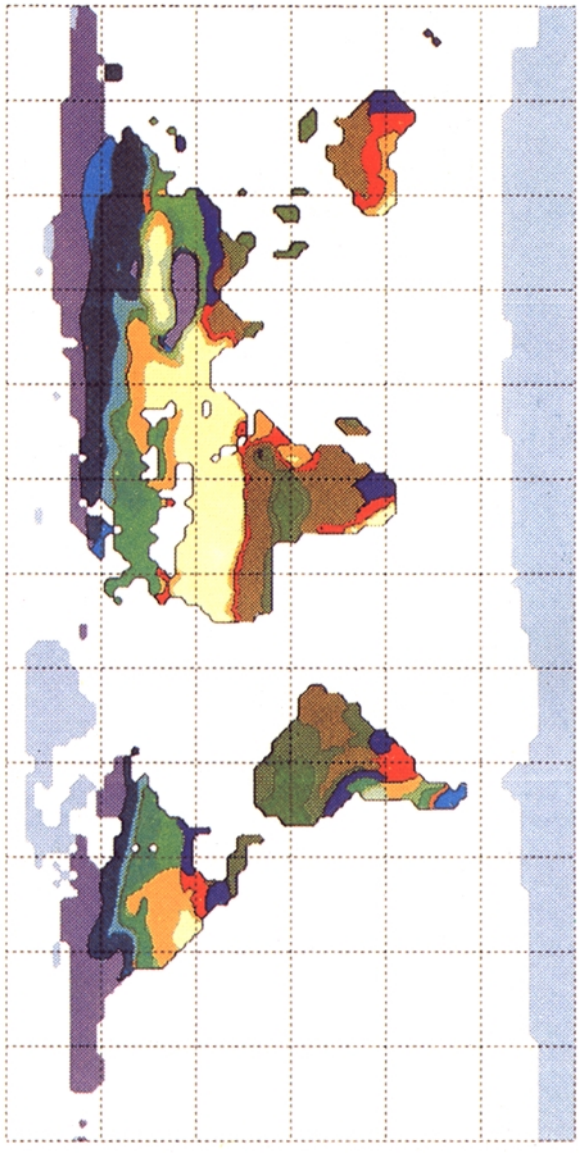

13(c) Present biome distribution computed from ECHAM3-T42 climatology.

Biome Modelling

The *biome model* of Prentice *et al.* (1992)[11], has been used to predict global patterns of potential natural plant formations, or biomes, from climatologies simulated by ECHAM. This study was undertaken in order to show the advantage of the biome model in diagnosing the performance of a climate model and assessing effects of past and future climate changes predicted by a climate model.

Good overall agreement is found between global patterns of biomes computed from observed and simulated data of present climate (Fig. 13a-c). However there are also major discrepancies indicated by a difference in biomes in Australia, in the Kalahari Desert, and in the central part of North America. These discrepancies can be traced back to errors in simulated rain fall as well as incorrect summer or winter temperatures.

Global patterns of biomes computed from an ice age simulation reveal that North America, Europe, and Siberia should have been covered largely by tundra and taiga, whereas only small differences are seen for the tropical rain forests. A potential North-East shift of biomes is indicated from a simulation with enhanced CO_2 concentration according to the IPCC Scenario A. Little change is seen in the tropical rain forests and the Sahara. Since the biome model used is not capable of predicting changes in vegetation patterns due to a rapid climate change, the latter simulation has to be taken as a prediction of changes in conditions favourable for the existence of certain biomes, not as a prediction of a future distribution of biomes (Claussen and Esch, 1992)[12].

Climate Sensitivity Experiments

Regional Simulation

Due to the limited computational resources, projections of the future climate have been performed so far with rather coarse models, typically T21 resolution. Consequently, the confidence in the simulated regional climate change is small. An economical alternative to improve regional climate prediction is to run a high-resolution atmospheric model for a particular region or even for the whole globe but for a limited period by using the SST changes predicted by the low-resolution coupled model. This so-called time-slice technique has been applied to the last 10 years of a 100-year climate projection using the ECHAM1-T21/LSG coupled model on the basis of the IPCC scenario A (Cubasch *et al.*, 1992)[13]. The AGCM used in these time-slice experiments is a T42 version of ECHAM3. In order to separate the impact of the higher resolution (T42 *vs.* T21) from the impact of modified physics (ECHAM3 *vs.* ECHAM1), a second experiment has been performed with ECHAM3 at T21 resolution. Preliminary results are:

- The climate response of ECHAM3/T42 forced with the SST changes predicted by the ECHAM1-T21/LSG coupled model is substantiasly different from that of the coupled model.
- The differences in the tropical precipitation signal (which is spatially more coherent in ECHAM3-T42) results mainly from a change in the convective

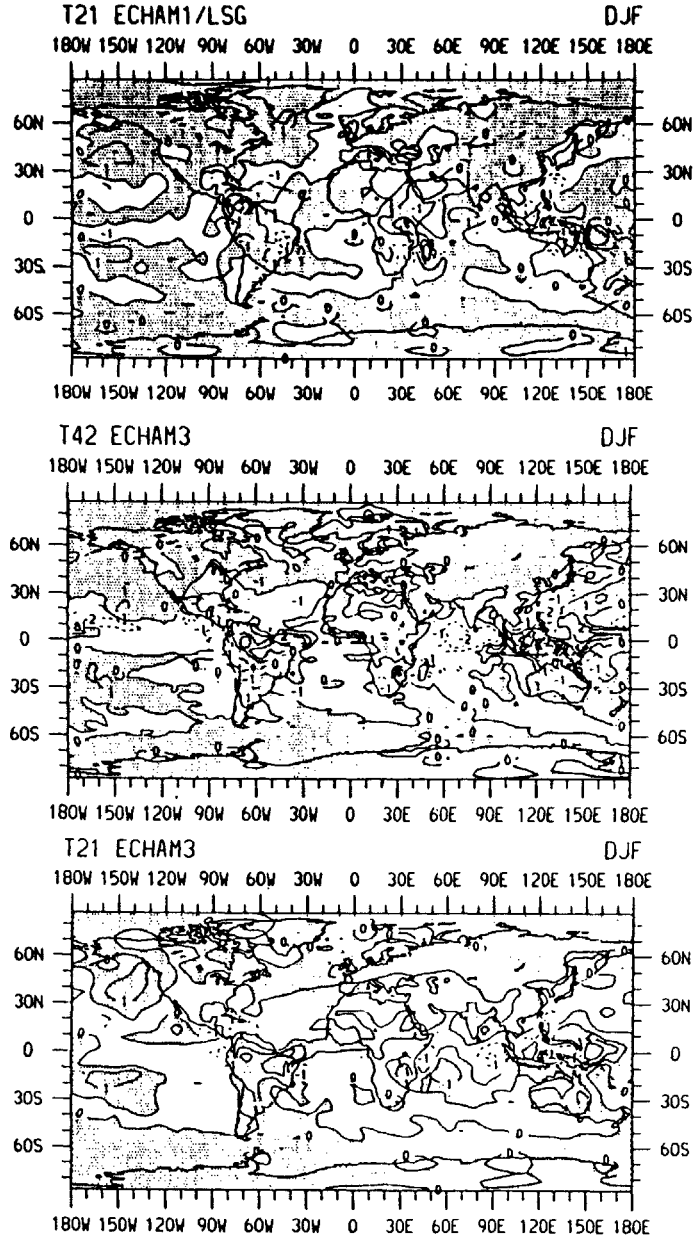

Fig 14 Change in precipitation with respect to the present winter (DJF) climate, as simulated for the last decade of a 100-year IPCC scenario A experiment.

Top: Coupled model T21 ECHAM1/LSG (10 years)

Middle and Bottom: ECHAM3 at T42 and T21 resolution, respectively forced with the SST change predicted by the couple model (30-year mean)

Contour spacing +/-1,2,4,8 mm/day. The stippling denotes areas with increased precipitation.

parameterization (mass-flux scheme in ECHAM3 *vs.* Kuo-scheme in ECHAM1) rather than from the higher resolution (Fig. 14).

- The substantial interdecadal variability in the T42 model (estimated from three 10-year realizations using the same SST forcing) does not allow to draw any firm conclusions concerning the risk of larger storm activity at middle latitudes, nor from any changes in the frequency of tropical storms.

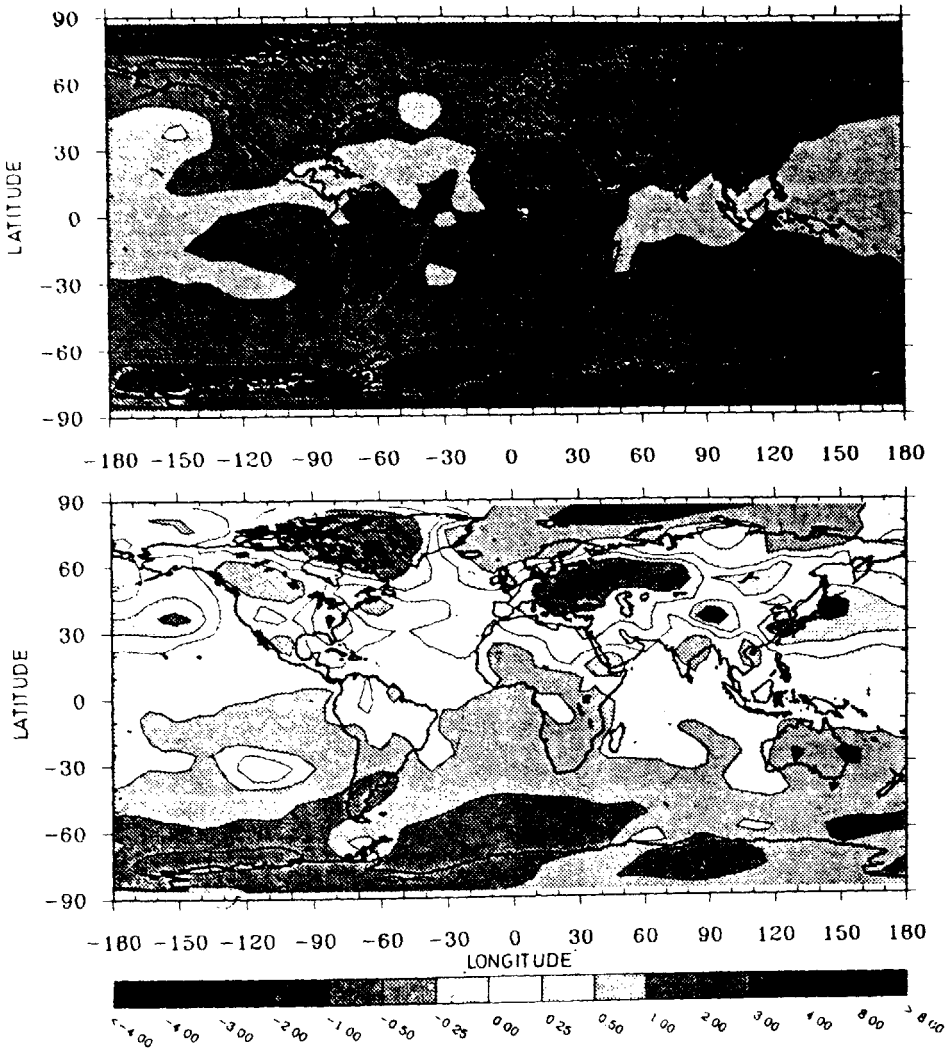

Fig 15 Equilibrium response of annual mean surface air temperature (°C) to different forcing assumptions since the beginning of the industrialization.

Top: Current greenhouse gas forcing corresponding to an effective CO^2 increase by 40% (2 Wm^{-2} in the global mean).

Bottom: Current greenhouse gas forcing as above and anthropogenic sulphate forcing (-0.7 Wm^{-2} in the global mean).

Sulphate Aerosol Forcing

In addition to atmospheric greenhouse gases, atmospheric aerosols can also affect climate. For example, biogenetic and anthropogenic sulphur species form sulphate-sulphate aerosol particles which exert a direct climatic effect due to backscattering of solar radiation and an indirect climatic effect by their ability to act as CCN (cloud condensation nuclei). Both effects tend to decrease global temperatures and may offset the global warming expected from anthropogenic greenhouse gas forcing. The hypothesis that past anthropogenic sulphur emissions have already changed our climate (Charlson *et al.*, 1991) is tested with the ECHAM1-T21 model coupled to a simple slab ocean model with a depth of 50m. In this study only the direct effect is addressed, i.e. a potential climate cooling resulting from backscattering of solar radiation by anthropogenic sulphate adopted from a simulation of the global sulphur cycle (Langner and Rodhe, 1991)[15]. The climate response is estimated by means of equilibrium runs with and without the sulphate forcing. Quasi-equilibrium is obtained after about 20 years of simulated time. In addition, a $2 \times CO_2$ forcing experiment has been performed and one which includes both effects, i.e. the current sulphate forcing and the current level of anthropogenic greenhouse gas forcing (approximately 2 W/m^2 according to IPCC estimates). The main conclusions are:

- The direct effect due to the backscattering of present-day anthropogenic sulphate aerosol is a global annual cooling of approximately 0.5°C. The cooling is stronger in the Northern Hemisphere (0.7°C) than in the Southern Hemisphere (0.3°C).
- The sulphate aerosol forcing is able to offset the current greenhouse warming over part of the Northern Hemisphere (Fig. 15).
- The equilibrium response to the sum of the current greenhouse gas forcing and anthropogenic sulphate is 0.5°C in the global annual mean, which is within the range of the observed warming during the last 100 years (0.4-0.7°C).

Global Transport Modelling

Using the semi-Lagrangian approach (Rasch and Williamson, 1990)[16], a transport code has been implemented in ECHAM3 which allows the handling of an arbitrary number of tracers. The subgrid-scale transport (vertical diffusion, convection) is treated analogously to the physical variables (heat and moisture). The code has been tested primarily with chemically inert short-lived and long-lived tracers such as radon or CFCs. Recently, the atmospheric part of the global sulphur cycle has been implemented in ECHAM. The simulation follows basically a scenario as described by Langner and Rodhe (1991)[15]: All emissions occur as DMS (dimethyl sulphide) and SO_2. The main source of SO_2 is anthropogenic emission by fossil fuel combustion and industrial activities. SO_2 is assumed to react with OH radicals producing H_2SO_4, and DMS react with OH producing SO_2. The aqueous phase oxidation of SO_2 is controlled by the oxidants H_2O_2 and O_3. SO_2 and SO_4 in clouds undergo wet removal by precipitation. The scavenging rate is assumed to be proportional to the model cal-

culated precipitation rates. The parameterization of dry deposition of all sulphur components is based on the turbulent transfer theory used in the GCM. Since the model does not include a chemical code, the distributions of OH, H_2O_2 and O_3 have to be prescribed from a chemical model.

The results (Fig. 16) are in good agreement with those obtained from Langner and Rodhe (1991)[15]. However, a comprehensive evaluation using observational data has not yet been performed.

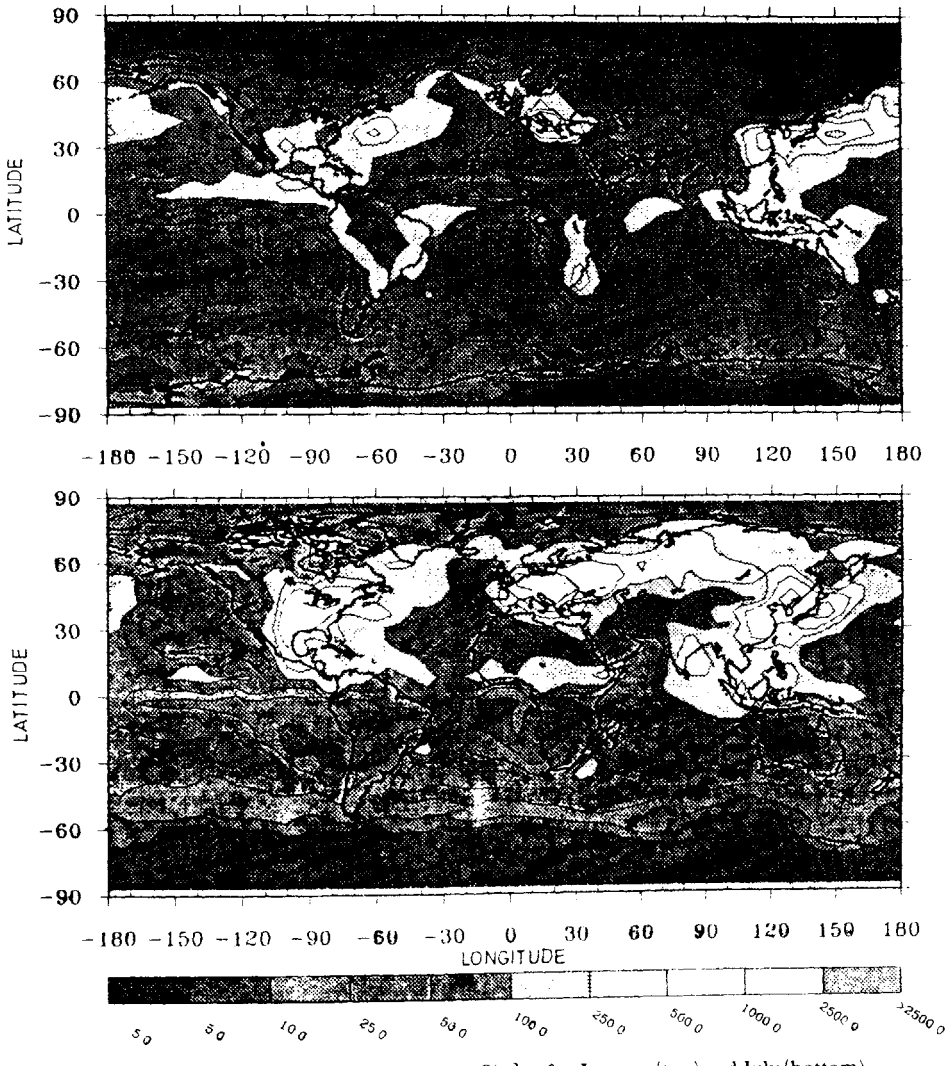

Fig 16 Dry and wet deposition of sulphur $mgS/m^2.yr$ for January (top) and July (bottom).

Acknowledgement

This article reviews the work of the staff and PhD students at MPI. We are particularly grateful for contributions by K Arpe, H Behr, R Budich, M Claussen, M Giorgetta, B Machenhauer and E Roeckner.

References

1 E Roeckner, K Arpe, L Bengtsson, S Brinkop, L Dümenil, M Esch, E Kirk, F Lunkeit, M Ponater, B Rockel, R Sausen, U Schlese, S Schubert and M Windelband Simulation ofthe present-day climate with the ECHAM model: impact of model physics and resolution. *Rep* No. 93, Max-Planck-Institut für Meteorologie Hamburg (1992) 178 pp.

1 (a) E Roeckner and M Ponater In: *ECMWF Seminar Proc Tropical-Extratropical Interactions* 467-480 (1991) Reading, U.K.

1 (b) E Roeckner, M Rieland and E Keup In: *ECMWF/WCRP Workshop Clouds, Radiative Transfer and the Hydrological Cycle* (1991) 199-222, Reading, U.K.

1 (c) E Roeckner *J exp Bot* **43** (1992) 1097-1109

2 M Claussen *Scale aggregation in semi-smooth flow Rep* No. 87. Max-Planck-Institut für Meteorologie (1992) 21 pp. (Submitted to: *J Hydrol*)

3 M Claussen and W Klaassen *Beitr Phys Atmos* **65** (1992) 243-248

4 A Stössel and M Claussen *Rep* No. 95 Max-Planck-Institut für Meteorologie 35 pp (1992) (*Accep)ted for Climate Dyn*)

4 (a) J T Houghton, G J Jenkins and J J Ephraums *Climate Change.* The IPCC Scientific Assessment. Cambridge University Press Cambridge (1990)

5 L Dümenil and E Todini In: *Advances in Theoretical Hydrology. A Tribute to James Dooge* (*Ed.* J P O'Kane) European Geophysical Society Series on Hydrological Sciences 1 Elsevier 253 pp

6 R Sausen, S Schubert and L Dümenil *Acc. J Hydrol*

7 L Dümenil, H -J Liebscher, U Schroeder, M Schumacher and K Wilke *Rep* No. 100, Max-Planck-Institut für Meteorologie Hamburg (1993)

8 U Lohmann, R Sausen, L Bengtsson, U Cubasch, J Perlwitz and E Roeckner, 1992 *Rep* No. 92 Max-Planck-Institute für Meteorologie Hamburg (1992) 22 pp.

8 (a) Y Mintz and V Serfafini

9 J O Dickey, S L Marcus and R Hide (*Accepted by Nature*)

10 L Dümenil and E Roeckner, 1992 In: *Simulation of Interannual and Intraseasonal Monsoon Variability. Rep Workshop,* National Center for Atmospheric Research, Boulder Colorado U.S.A. (1992). World Climate Research Programme WCRP-68 WMO/TD-No. 470

11 I C Prentice, W Cramer, S P Harrison, R Leemans, R A Monserud and A M Solomon *J Biogeograph* **19** (1992) 117-134

12 M Claussen and M Esch *Rep* No. 89, Max-Planck-Institut für Meteorologie (1992) 19 pp. (*Acc publ Climate Dyn*)

13 U Cubasch, K Hasselmann, H Höck, E Maier-Reimer, U Mikolajewicz, B D Santer and R Sausen *Climate Dyn* **8** (1992) 55-69

14 R J Charlson, J Langner, H Rodhe, C B Leovy and S G Warren *Tellus* **3** AB (1991) 152-163

15 J Langner and H Rodhe *J atmos Chem* **13** (1991) 225-263

16 P J Rasch and D Williamson *Models of the atmosphere, QJR Meteorol Soc* **116** (1990) 1071-1090